*Biochimica et Biophysica Acta*, 944 (1988) 63–72
Elsevier

BBA 74117



# Passive ion permeability of lipid membranes modelled via lipid-domain interfacial area

Leonor Cruzeiro-Hansson [a] and Ole G. Mouritsen [b]

[a] *Laboratory of Applied Mathematical Physics and* [b] *Department of Structural Properties of Materials, The Technical University of Denmark, Lyngby (Denmark)*

(Received 20 April 1988)

Key words: Lipid bilayer; Phase transition; Computer simulation; Density fluctuation; Ion permeability; Reversible electrical breakdown

**A microscopic interaction model of the gel-to-fluid chain-melting phase transition of fully hydrated lipid bilayer membranes is used as a basis for modelling the temperature dependence of passive transmembrane permeability of small ions, e.g. $Na^+$. Computer simulation of the model shows that the phase transition is accompanied by strong lateral density fluctuations which manifest themselves in the formation of inhomogeneous equilibrium structures of coexisting gel and fluid domains. The interfaces of these domains are found to be dominated by intermediate lipid-chain conformations. The interfacial area is shown to have a pronounced peak at the phase transition. By imposing a simple model for ion diffusion through membranes which assigns a high relative permeation rate to the domain interfaces, the interfacial area is then identified as a membrane property which has the proper temperature variation to account for the peculiar experimental observation of a strongly enhanced passive ion permeability at the phase transition. The excellent agreement with the experimental data for $Na^+$-permeation, taken together with recent experimental results for the phase transition kinetics, provides new insight into the microphysical mechanisms of reversible electric breakdown. This insight indicates that there is no need for aqueous pore-formation to explain the experimental observation of a dramatic increase in ion conductance subsequent to electric pulses.**

## Introduction

Ion transport in biological membranes is predominantly mediated by specific protein channels or ion pumps which selectively direct the ionic current across the membranes [1]. The lipid bilayer matrix of the membrane is by itself, however, not impermeable to ions which can passively diffuse through the bilayer in an ion-specific way [2]. A particularly striking observation was made some years ago by Papahadjopoulos et al. [3] who measured a dramatic peak–rather than a discontinuous increase–of the passive $Na^+$-permeability through vesicles of dipalmitoylphosphatidylcholine (DPPC) near the gel-to-fluid phase transition at $T_m = 314$ K. Obviously, biological membranes do not suffer from such anomalous behaviour and other membrane components, e.g. cholesterol [4], often function so as to seal the membranes. Still, a description of the mechanisms responsible for the thermal peak in the passive ion permeability in lipid bilayers is important for a general understanding of membrane structure and dynamics.

In this paper we provide quantitative theoretical support to the idea, first advanced by Papa-

Correspondence: O.G. Mouritsen, Department of Structural Properties of Materials, The Technical University of Denmark, Building 307, DK-2800 Lyngby, Denmark.

hadjopoulos et al. [3] and later investigated by several other workers [5–11], that the permeability peak at $T_m$ for certain ions and molecules may be related to specially leaky interfacial regions between gel and fluid lipid domains which are formed near the phase transition. By using a rather realistic microscopic interaction model of the phase transition and by simulating the numerically exact properties of this model, taking full account of the thermal fluctuations of the many-particle correlations, we show for the first time quantitatively that the temperature variation of the interfacial area may be the key property for describing the peak in the passive ion permeability. Our approach should be considered as a kind of minimal model description involving the fewest possible assumptions. It furthermore provides a basis for discussing the microphysical phenomena underlying electric-field effects on membranes, such as reversible electrical breakdown and subsequent irreversible mechanical breakdown. We conclude from this discussion that there is no need for invoking aqueous pores to describe either the anomalous ion permeability or the phenomenon of reversible electric breakdown in lipid membranes.

## 2. Model of phase transition and simulation techniques

Our numerical calculations of the lipid membrane properties near the gel-to-fluid phase transition are based on the ten-state model due to Pink and collaborators [12,13]. This model has had considerable success in describing bulk thermodynamic and spectroscopic experimental data for pure lipid bilayers [12–14] as well as effects of lipid–protein [15–17] and lipid–cholesterol interactions [18] in lipid membranes. Furthermore, extensive computer-simulation studies of this model have shown that the first-order phase transition is accompanied by lateral density fluctuations of an intensity which resembles pseudo-critical phenomena [19–21], also in accordance with a variety of experimental studies using different techniques [22–25].

The 10-state model [12] is a pseudo-two-dimensional lattice model which neglects the translational modes of the lipid molecules [26] and focuses on the conformational degrees of freedom of the acyl chains. The conformational chain states and their statistics are the main determinants of the equilibrium properties of the phase transition which predominantly is a chain-melting transition. The model is formulated in terms of ten conformational states, of which one is the fully ordered all-*trans* conformation and one is a highly excited fluid state which is characteristic of the high-temperature thermodynamic fluid phase ($f$). The eight remaining states are intermediate chain states which may be viewed as low-energy excitations of the all-*trans* state. These eight states together with the all-*trans* state are all characteristic of the thermodynamic gel phase ($g$). The interactions between the acyl chains are modelled by anisotropic van der Waals forces, and the model furthermore includes an internal lateral pressure to assure interfacial stability. The values of the various model parameters are the same as those used in earlier simulation studies of the ten-state model for DPPC bilayers [14,19,20].

The statistical mechanical and thermodynamic properties of the model are calculated numerically by Monte Carlo computer-simulation techniques [27]. By these techniques, which fully allow for the thermal fluctuations in a many-particle system, very accurate numerical statistics are sampled for the microconfigurations typical of the model for any given set of thermodynamic parameters, in the present case the temperature. From these statistics, the thermodynamic properties are readily derived as functions of temperature. Furthermore, and more importantly for the present problem, the simulations give access to the spatial structure of the microconfigurations and thus permit possible membrane heterogeneity and domain formation to be revealed directly. Any such heterogeneity is thus derived from first principles and is not a consequence of any initial assumption.

The calculations are carried out on triangular lattices with $N = L \times L$ lattice points. An acyl chain is positioned at each lattice site. The system is subject to periodic boundary conditions in order to minimize the effects of finite size. A series of different lattice sizes, $N = 400$, 1600, and 10000, is studied systematically in order to evaluate such possible size effects. Precautions are taken so as to

ensure that the statistics generated correspond to thermodynamic equilibrium [27].

## 3. Clusters and interfaces

In Fig. 1 is shown a series of snapshots of microconfigurations typical for temperatures on both sides of the phase transition temperature, $T_m$. The figure, which distinguishes between chains in gel states (the nine low-lying states) and chains in the fluid state, clearly shows that the thermally induced lateral density fluctuations lead to an instantaneously heterogeneous membrane structure: below $T_m$, clusters of the fluid phase (i.e. of chains in the fluid conformational state) are formed in the gel matrix (i.e. in a sea of chains in the all-*trans* or the intermediate conformational states); above $T_m$, clusters of the gel phase (i.e. chains in all-*trans* or intermediate states) are formed in the fluid matrix (i.e. the phase of chains in the fluid state). These clusters are dynamic entities and they fluctuate in position and size. Nevertheless, they are described by an equilibrium distribution function $n_l^\alpha(T)$ [20], $\alpha = g, f$, where $n_l^\alpha$ denotes the number of $\alpha$-clusters (or domains) encompassing $l$ lipid chains. The clusters are defined via a nearest-neighbour connectivity criterion consistent with the nearest-neighbour chain-chain interaction range. The distribution function has a tail towards the larger clusters which raises as $T_m$ is approached from either side. The average cluster size is then obtained as

$$\bar{l}(T) = \sum_l l n_l^\alpha(T) \Big/ \sum_l n_l^\alpha(T) \tag{1}$$

where $\alpha = f$ in the gel phase and $\alpha = g$ in the fluid phase. The results for $\bar{l}$ are shown in Fig. 2 which shows that $\bar{l}$ has a dramatic peak at $T_m$. The figure includes data for different system sizes and demonstrates that the large system with $N = 10000$ chains without any doubt represents the thermodynamic limit ($N \to \infty$) as far as the cluster statistics are concerned. In the rest of the paper we shall therefore refer to data obtained exclusively for the $N = 10000$ system.

It should at this point be mentioned that the inhomogeneous membrane states pictured in Fig. 1 for $T \neq T_m$ do not correspond to two-phase coexistence in the thermodynamic sense. For a one-component system, Gibbs' phase rule forbids this except at $T = T_m$. The clusters of the opposite phase formed by density fluctuations in the equilibrium bulk background phase are not macroscopic entities and they are stabilized by the interplay between configurational entropy and interfacial free energy.

In order to quantitatively characterize the bilayer heterogeneity as pictured qualitatively in Fig. 1, we divide the membrane plane into three regions: the background matrix (the bulk), the clusters, and the interface between the clusters and the bulk. The thermalization of the system within the

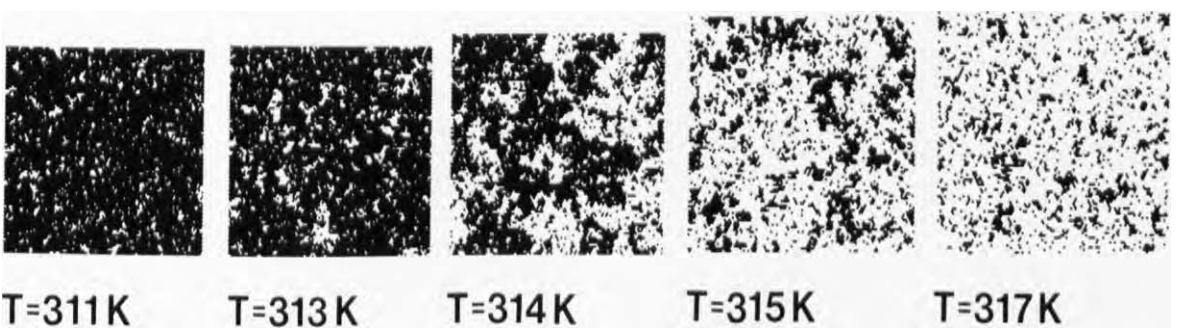


Fig. 1. Snapshots of microconfigurations typical of a series of temperatures around the lipid bilayer gel-to-fluid phase transition. $T_m = 314$ K. The system contains 10000 acyl chains of DPPC on a triangular lattice and the lattice parameter has been scaled so as to display the lateral expansion of the bilayer as the temperature is increased. Black symbols denote lipid acyl chains in gel conformations (all-*trans* and intermediate states) and blank areas denote chains in the fluid conformational state. The figure clearly shows the cluster formation in the phase transition region.

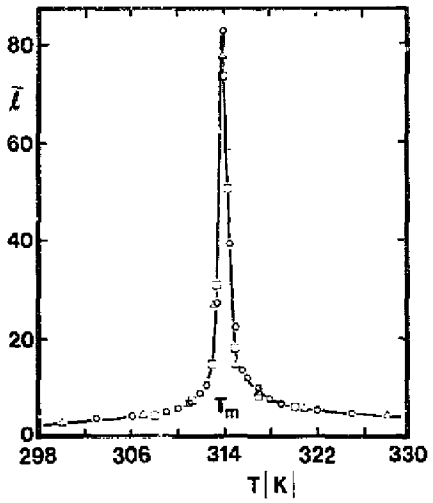


Fig. 2. Average cluster size, $\bar{l}(T)$ Eqn. 1, as a function of temperature for lipid membrane models of different sizes. $N = 400$ (△), $N = 1600$ (□), and $N = 10000$ (○) acyl chains. The model parameters are pertinent for DPPC. The lower cut-off cluster size was chosen to be three chains for this figure.

computer simulation is technically performed by coupling the system to a heat bath by stochastic single-chain excitations [27]. In order to exclude very localized random events which arise due to this stochastic dynamics, we have chosen (somewhat arbitrarily) to only consider clusters which contain more than about fourteen chains (i.e. seven DPPC molecules in e.g. a hexagon) for our cluster

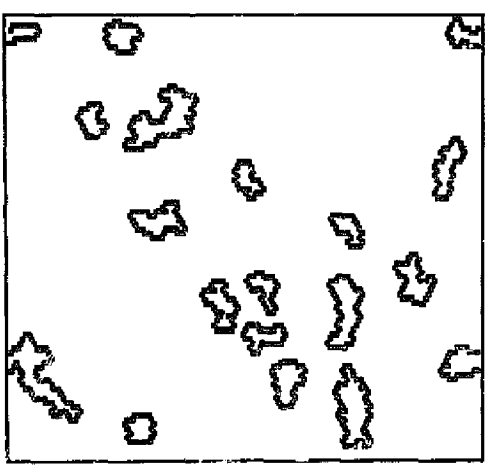

Fig. 3. Snapshot of the microconfiguration for a lipid bilayer system with 10000 chains at $T = 312$ K. Only the interfacial region is shown.

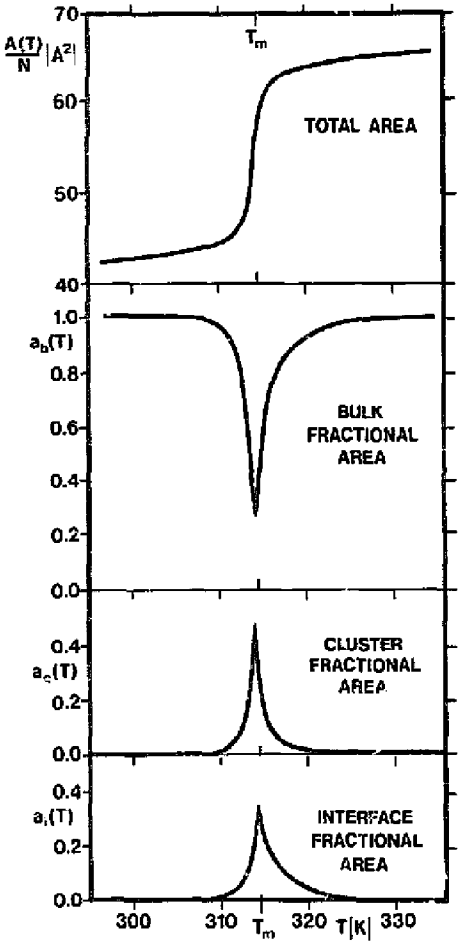


Fig. 4. Temperature dependence of total membrane area per molecule and fractional areas of the membrane in the bulk, in the clusters, and in the interfaces. The interface is defined as the first interfacial layer of lipid chains.

analysis. The results we report below are only slightly sensitive as to how this lower cut-off is actually chosen. The cluster-bulk interface is now probed via a series of molecular layers. The first layer is defined as those chains which are connected by nearest-neighbour bonds to the cluster boundary, the second layer as those chains which are nearest-neighbours to the first layer, etc. As an example, Fig. 3 illustrates how the interfacial region, given as the first layer, is typically distributed at $T = 312$ K.

With the above definitions of the three membrane regions, the membrane heterogeneity as a function of temperature may be described by the

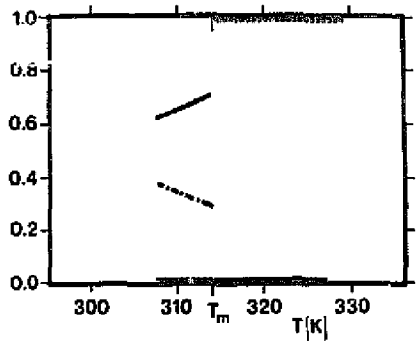


Fig. 5. Relative occurrence of all-*trans* (·–·–·), intermediate (———), and fluid (- - - - -) chain-conformational states of the first interfacial layer. Due to the cluster definition the occurrence of the fluid state is zero below $T_m$ and unity above $T_m$. Similarly, there is no intermediate gel states in the first interfacial layer of gel clusters above $T_m$.

relative amounts of the membrane area in the three regions. Fig. 4 shows the results in the case of the interface being defined as the first layer of chains. This figure also shows the temperature variation of the total membrane area per molecule, $A(T)/N$. There is a clear tendency for the cluster fractional area to increase strongly around $T_m$. Simultaneously, the interfacial area has a distinct peak at $T_m$. The peak in the cluster area is less broad than the peak in the interfacial area because the increase in cluster area is accomplished by an increase in the average size of the clusters (cf. Fig. 1) and not through a proliferation of small clusters. This observation has important consequences for the ion permeability.

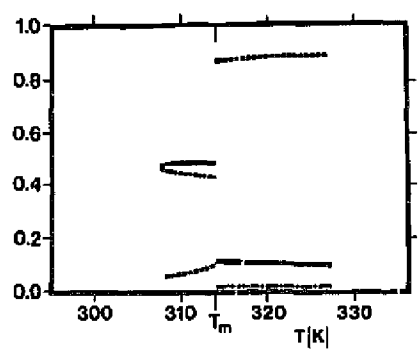


Fig. 6. Relative occurrence of all-*trans* (·–·–·), intermediate (———), and fluid (- - - - -) chain-conformational states of the second interfacial layer.

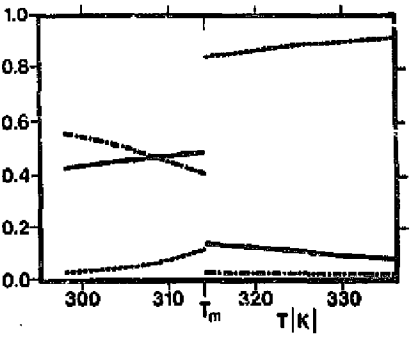


Fig. 7. Relative occurrence of all-*trans* (·–·–·), intermediate (———), and fluid (- - - - -) chain-conformational states in the bulk.

The question now arises whether the interfacial region has certain characteristics regarding the chain-conformational states. This question is explored in Figs. 5 and 6 which show the relative occurrence of all-*trans*, intermediate, and fluid chain-conformational states of the chains constituting the first (Fig. 5) and second (Fig. 6) interfacial layers, respectively, as compared with the bulk (Fig. 7). These figures demonstrate unequivocally that the first interfacial layer is strongly dominated by chains in intermediate conformational states. Conversely, the occurences of the states in the second interfacial layer are close to the values for the bulk. This is a very conspicuous finding which gives strong quantitative support to previous conjectures [19]. It shows that the interface is soft, although rather sharp and well-localized in space, and it acts as a sink for excited gel-like chain conformations. In the following sections we shall relate this special interfacial environment to the transport properties of the lipid bilayer.

## 4. Model of passive ion transport

In line with the work of Kanehisa and Tsong [7] we propose a simple model of passive ion diffusion across membranes. The model assumes that the bulk and cluster regions of the membrane each have their characteristic rates of diffusion which both are less than the diffusion rate in the interface. In the case of a liposome of volume $V(T)$ with a certain internal ion concentration,

$c(t) = N(t)/V(T)$, the number $dN(t)$ of ions leaving the liposome at time $t$ can be expressed as

$$dN(t) \propto c(t)v(T)A(T)P(T)\,dt \tag{2}$$

where $v(T)$ is the velocity of the impinging ion, $A(T)$ is the internal area of the liposome, and $P(T)$ is the probability that an ion crosses the membrane once it hits it. From the kinetic theory we know that the velocity of the ions has a Maxwellian distribution and hence $v(T) = (k_B T/2\pi m)^{1/2}$ where $m$ is the ion mass. Substitution of this expression for $v(T)$ into Eqn. 2 gives

$$dN(t) \propto CA(T)^{-1/2}N(t)T^{1/2}P(t)\,dt \tag{3}$$

with

$$C = 3\left(\frac{2k_B}{m}\right)^{1/2} \tag{4}$$

We shall now assume that the probability, $P(T)$, of an ion crossing the membrane can be written as a sum of three terms

$$P(T) = a_b(T)p_b + a_c(T)p_c + a_i(T)p_i \tag{5}$$

where $a_b$, $a_c$, and $a_i$ are the fractions of the membrane area occupied by the bulk, the clusters, and the interfaces, respectively. $p_b$, $p_c$, and $p_i$ denote the corresponding regional probabilities of transfer. As indicated by Eqn. 5 only the area fractions, $a$, are considered to be temperature dependent. This is in contrast to the approach by Kanehisa and Tsong [7] who take the area fractions as well as the regional probabilities to depend on temperature. Integration of Eqn. 3 then leads to the simple expression for the fraction, $f(t)$, of ions retained in the liposome

$$f(t,T) = \frac{N(t)}{N(t=0)} = \exp(-CA(T)^{-1/2}T^{1/2}P(T)t) \tag{6}$$

In the work by Papahadjopoulos et al. [3] it is the fraction, $1 - f(t)$, of ions leaving the liposome which is measured.

## 5. Temperature dependence of passive ion permeability: comparison with experiments

Using the simple model of passive ion transport of Section 4, viz. Eqns. 5 and 6, we can now predict the temperature variation in the passive ion permeability by inserting into Eqn. 5 the computer-simulation results of Section 3 for the fractions of the membrane areas, $a_b(T)$, $a_c(T)$, and $a_i(T)$, occupied by the bulk, the clusters, and the interfaces (cf. Fig. 4). This calculation requires values of the so far unknown temperature-independent regional transfer probabilities, $p_b$, $p_c$, and $p_i$. We have at present no way of calculating these numbers from basic principles and similarly we are not aware of any pertinent experimental results. Consequently, we are left with these three parameters to be fitted to the experimental data for the global permeability. However, we are going to impose a constraint by assuming that the interfacial area is associated with a very high relative regional permeability, $p_i \gg p_b$, $p_c$. This assumption is motivated by the presence of high defect density in the interfacial region which is likely to lead to bad packing and leakiness.

To facilitate the comparison with the experiments of Ref. 3 we focus on the quantity $\log f(t)$ and normalize the theoretical as well as the experimental results relative to the results at a selected temperature, $T = 298$ K. Hence we study the ratio

$$R(T) = \frac{\log f(T)}{\log f(T=298)} = \frac{A(T)^{-1/2}T^{1/2}P(T)}{A(298)^{-1/2}(298)^{1/2}P(T=298)} \tag{7}$$

which we refer to as the relative permeability. In Fig. 8 are shown the experimental results [3] for $R(T)$ in the case of $Na^+$-permeation compared with the theoretical prediction. In the theoretical calculation we have used $p_i = 1$ and ($p_b$, $p_c$ = 0.0066, 0.11) below $T_m$ and (0.11, 0.0066) above $T_m$. The overall fit to the experimental data is rather satisfactory considering the considerable uncertainty in the experimental data, in particular above $T_m$ [3]. The details of the fit are, however, sensitive to the values chosen for the regional transfer probabilities, whereas the overall shape of the curve is not as long as $p_i \gg p_b$, $p_c$. The precise values of the regional transfer probabilities are peculiar to the specific type of ion in question. The lower cut-off in cluster size used for determining the interfacial area, $a_i$ Fig. 4, also has some influence on the width of the theoretical peak. We

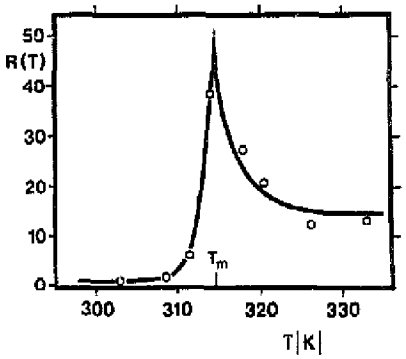


Fig. 8. Relative permeability, $R(T)$ Eqn. 7, of $Na^+$ ions in liposomes as measured by radioactive $^{22}Na$-techniques (○) and as calculated theoretically in the present paper using the temperature variation of the interfacial area (———). The experimental data are reproduced from the work of Papahadjopoulos et al. [3]. The permeability scale is in this representation chosen relative to the experimental value of the permeability at $T = 298$ K.

conclude from Fig. 8 that the minimal model of passive ion diffusion in combination with accurate numerical data for the interfacial area near the lipid-bilayer main phase transition is capable of accounting for the striking thermal anomaly in passive $Na^+$-permeability.

## 6. Reversible electric breakdown

In addition to the thermal anomaly, another type of anomalous behaviour in the permeability of membranes is observed when electric pulses of short duration are applied to the membrane [28,29]. On the basis of the results presented above on cluster formation and its relation to passive ion transport we shall in this section examine a possible relationship between the two types of anomalous behaviour. In the case of a voltage between 0.6 and 1 V, corresponding to an electric field of $(2–3) \cdot 10^6$ V · cm$^{-1}$, applied over a period of $0.5 \cdot 10^{-6}$ s, a decrease within $10^{-8}$ s of membrane resistance of up to a factor of $10^9$ is observed. This striking phenomenon is called reversible electric breakdown (REB). In pure lipid bilayer membranes REB is followed by irreversible (mechanical) breakdown by which the membrane ruptures irreversibly within a period of $10^{-3}$ s or longer [30]. However, oxidized cholesterol membranes and lipid bilayers with high cholesterol content show REB only [28,29].

The interpretation of REB has conventionally been closely connected with that of irreversible (mechanical) breakdown. The latter being easily rationalized as the result of aqueous-pore formation, REB is also thought to be due to ion diffusion through aqueous pores which are either considered to be induced directly by the electric field [28,31] or enhanced from a pre-existing population of thermally induced small pores [32–34]. While a permanent population of aqueous pores is hard to justify on energetic grounds [35] and seems contradictory to the high resistance of unperturbed lipid bilayers and what is known about bilayer structure and dynamics, an electrically induced population is not without problems either. Although it is possible and indeed quite probable that a sufficiently prolonged electric pulse induces aqueous pores, the kinetics of REB seems too fast, i.e. it is hard to imagine the formation of such pores in a time less than $10^{-8}$ s which is the time it takes for the membrane resistance to drop by a factor of $10^9$ [28].

We are here going to argue, together with Abidor et al. [30], that irreversible breakdown and REB, although causally related (i.e. the latter always precedes the first), are two different processes of different kinetics. This point of view gets strong support from recent experimental studies of lipid membrane phase-transition kinetics. Holzwarth and coworkers [36], using a laser temperature-jump technique which within less than $10^{-9}$ s induces a 1 K change in the lipid bilayer temperature, detected via a turbidity measurement the existence of five separate relaxation times in the time range from $10^{-9}$ to $10^{-3}$ s. Holzwarth interpreted these findings in terms of five kinetic processes in the bilayer: (i) Rotational isomerization (e.g. kink formation) of the acyl chains, $\tau_1 \approx 4 \cdot 10^{-9}$ s. (ii) Chain-length and headgroup-dependent bilayer expansion via headgroup rotation, $\tau_2 \approx 3 \cdot 10^{-7}$ s. (iii) Lateral diffusion and onset of cooperative interactions, $\tau_3 \approx 10^{-5}$ s. (iv) Cluster formation, $\tau_4 \approx 3 \cdot 10^{-4}$ s. (v) Melting of clusters, $\tau_5 \approx 3 \cdot 10^{-3}$ s. Holzwarth [36] also studied the effect of cholesterol, protein, and polypeptides on the different relaxation processes and found that the processes (i) and (ii) were not altered but that (iv)

and (v) were strongly suppressed by cholesterol and almost eliminated by gramicidin-A and bacteriorhodopsin. These kinetic data discredit the possibility that a deformation like the one needed for aqueous-pore formation can occur on a time scale shorter than $10^{-8}$ s. Instead, if we consider the coupling of an electric field to the different kinetic processes, then REB, taking place in less than $10^{-8}$ s, involves at most the two fastest processes (i) and (ii). On the other hand, irreversible breakdown, which takes place on the scale $10^{-3}$ s, can be related to the cluster-formation process (iv) which is the process most likely to induce large-scale heterogeneity in the membrane.

On the basis of the above considerations, we propose the following interpretation of the phenomena following the application of electric pulses to lipid bilayers. First, processes (i) and (ii) are activated and REB is associated with these processes which take place on a time scale between $10^{-9}$ and $10^{-7}$ s. Second, and much later on a scale of $10^{-3}$ s, processes (iv) and (v) come into play and generate large-scale hydrophobic defects which develop into aqueous pores and irreversible breakdown. This proposal explains the kinetics of REB and irreversible breakdown. It furthermore explains the fact that cholesterol-containing lipid bilayers survive REB simply because processes (iv) and (v) are inhibited by large amounts of cholesterol and cluster formation will not take place. The lack of cooperativity and cluster formation is moreover consistent with recent progress obtained in understanding the lecithin-cholesterol phase diagram [18].

The ideas underlying our proposal can be subjected to experimental tests. For example, it could be investigated whether other membrane components, in addition to cholesterol and the proteins already studied which suppress membrane processes related to cluster formation, permit REB but prevent irreversible breakdown.

The kinetic studies by Holzwarth [36] are in perfect accordance with the cluster formation seen in the computer simulation of the ten-state model of the lipid bilayer gel-to-fluid phase transition as discussed in Section 3, although computer simulations of the Monte Carlo type do not permit an absolute determination of the various time scales [27]. Following the interpretation of REB suggested in the present section, we suggest a parallel interpretation of the increased passive ion permeability at the phase transition as being due to increased intensity of the fast kinetic processes (i) and (ii) in the interfacial region where there is a high relative occurrence of intermediate acyl-chain conformational states (kinks and jogs). Hence the two types of lipid membrane anomalies in the ionic conductance are caused essentially by the same mechanism and there is no need to invoke aqueous-pore formation in any of the two cases. We therefore conclude that a proper model of passive ion transport in lipid bilayers must be able to account for increases in permeability due to rotational isomerization via *gauche* bond formation and membrane expansion.

## 7. Conclusions

Lipid bilayers are generally characterized by very low permeability to small ions such as $Na^+$ and $K^+$. An anomalous result was first obtained by Papahadjopoulos et al. [3] who found a dramatic peak – rather than a monotonic increase – of the permeability of $Na^+$ at the phase transition of lipesomes, cf. Fig. 8. Papahadjopoulos et al. explained this striking phenomenon as being caused by coexistence of gel and fluid domains near the phase transition. The interface which is formed by this mechanism should then permit leakage of the ions. This explanation was later questioned by other authors [6,8] who argued that such interfaces could not exist on thermodynamic grounds. Yet still others [2,5] proposed that the peak is a result of enhanced lateral density fluctuations. As we have seen in the present work, membrane heterogeneity and the formation of dynamic interfaces will indeed take place (cf. Figs. 1 and 3) and are mere consequences of the diversity of lipid-chain conformations and their thermal cooperative fluctuations. The interfaces are stabilized kinetically by the intermediate lipid-chain conformations [19]. It is difficult to provide a direct experimental verification of the existence of clusters in a lipid membrane due to problems with time resolution of the fluctuation clusters. Recent careful analysis of fluorescence lifetime heterogeneity [25] has been interpreted in terms of gel clusters above the phase transition. The most con-

vincing indication of cluster formation is indirect and comes from analyses of bulk fluctuating quantities in terms of membrane softening [20] and pseudo-critical behaviour [22–25].

We have in this work related the temperature dependence of the interfacial area to the passive ion permeability via a simple model of ion diffusion. The model has proved capable of reproducing the experimental data for permeation of $Na^+$-ions across liposomes, cf. Fig. 8. We therefore believe it contains the essential physics for characterizing the passive permeability. The model should be considered a minimal model in the sense that it incorporates the fewest possible assumptions about the diffusion mechanism. It has considerably fewer free parameters to fit than previous approaches focusing on the special importance of the interface between fluid and gel domains [3,7]. Formation of dynamic clusters and interfaces is related to lateral density fluctuations and lateral bilayer compressibility. Still, our approach is conceptually different from the approach which directly relates the permeability to the global lateral density fluctuations, $\Delta A^2(T)$, via a standard Eyring rate proportional to $\exp(-\epsilon\Delta A^2(T)/k_BT)$ [2,5,6,13]. In our view, it is the local event of formation of an interface of defects rather than the global fluctuation in area which is linked to enhanced ion permeation. It is, however, not possible, considering (i) the limited accuracy of the experimental data currently available for e.g. $Na^+$-permeation [2,3] and (ii) the persisting parameters of the theoretical models, to rule out the validity of either of the approaches.

The approach taken in the present work suggests that it is the special nature of the interfacial regions, e.g. the structural defects and the mismatch in molecular packing, which is responsible for the leakiness and enhanced permeation of ions near the phase transition. This suggestion is not restricted to the permeation of $Na^+$-ions but should have a more general sphere of applicability to other ions and molecules. This is in line with the ideas put forward by other workers [7,10] and it is furthermore corroborated by the experimental observation of permeability peaks for e.g. other alkali metal ions [2,11], TEMPO (2,2,6,6-tetramethylpiperidinyl-1-oxy)choline [10], ANS (8-anilino-1-naphthalinesulfonate) [7], and water [37]. Similarly, the lateral heterogeneity implied by the interfaces formed in binary lipid mixtures would facilitate transport of matter [8,38,39]. In biological membranes, interfacial regions could possibly facilitate the insertion of newly synthesized proteins and lipids [38]. The width of the permeability peak predicted for the various substances would depend on the size of the defect required for passage, i.e. within our model it would depend on the lower cut-off for the cluster size. It is reassuring to note that a larger cut-off leads to sharper peaks, in accordance with the experimental finding for the large ANS-molecule [7].

The enhanced ion permeability near the lipid membrane phase transition can be suppressed by cholesterol [3] in sufficient concentration. Since cholesterol in high concentrations eliminates the phase transition, lowers the area compressibility, and leads to more mechanically stable and cohesive membranes [4,40], it is likely that it will inhibit permeation in general. Preliminary computersimulation results (Mouritsen, O.G., Hjort Ipsen, J. and Cruzeiro-Hansson, L., unpublished data) show that cholesterol is distributed inhomogeneously in the membrane plane and is predominantly found at the gel-fluid interfaces of the clusters formed near the phase transition. This finding is consistent with fluorescence microscopy studies of lipid monolayers where it was found that cholesterol stabilizes solid-liquid interfaces [41]. This changes the structure of the interfaces and may explain the suppression of the permeability peak.

Finally, we wish to point out that the approach to passive transport described in the present work does not assume a specific microscopic physical mechanism by which the transport is actually performed. Such molecular mechanisms have been previously proposed for passive transport along the lipid hydrocarbon chains, both invoking quantum-mechanical tunnelling [42] and classical kink-defect carriers [43].

## Acknowledgements

This work was supported by the Danish Natural Science Research Council under grant J. nr. 5.21.99.72. One of the authors (L.C.-H.) acknowl-

edges the support of the C. Gulbenkian Foundation, Lisbon, Portugal.

## Note added in proof (Received 8 August 1988)

Biltonen (Biltonen, R., personal communication) has pointed out that the cluster size distribution function (Fig. 2) obtained from the microscopic interaction model used in this work is quantitatively similar to that obtained experimentally [44] from scanning calorimetric data, without assuming a particular model of the chain-melting transition (see Fig. 2 of Ref. 44).

## References


1 Eisenman, G. and Dani, J.A. (1987) Annu. Rev. Biophys. Biophys. Chem. 16, 205–226.
2 Georgallas, A., MacArthur, J.D., Ma, X.-P., Nguyen, C.V., Palmer, G.R., Singer, M.A. and Tse, M.Y. (1987) J. Chem. Phys. 86, 7218–7226.
3 Papahadjopoulos, D., Jacobsen, K., Nir, S. and Isac, T. (1973) Biochim. Biophys. Acta 311, 330–348.
4 Evans, E. and Needham, D. (1986) Faraday Discuss. Chem. Soc. 81, 267–280.
5 Doniach, S. (1978) J. Chem. Phys. 68, 4912–4916.
6 Nagle, J.F. and Scott, H.L. (1978) Biochim. Biophys. Acta 513, 236–243.
7 Kanehisa, M.I. and Tsong, T.Y. (1978) J. Am. Chem. Soc. 100, 424–432.
8 Marčelja, S. and Wolfe, J. (1979) Biochim. Biophys. Acta 557, 24–31.
9 Lawaczek, R., Kainosho, M., Girardet, J.-L. and Chan, S.I. (1975) Nature 256, 584–586.
10 Marsh, D., Watts, A. and Knowles, P.F. (1976) Biochemistry 15, 3570–3578.
11 Blok, M.C., Van der Neut-Kok, E.C.M., Van Deenen, L.L.M. and De Gier, J. (1975) Biochim. Biophys. Acta 406, 187–196.
12 Pink, D.A., Green, T. and Chapman, D. (1980) Biochemistry 19, 349–356.
13 Caillé, A., Pink, D.A., De Verteuil, F. and Zuckermann, M.J. (1980) Can. J. Phys. 58, 581–611.
14 Mouritsen, O.G., Boothroyd, A., Harris, R., Jan, N., Lookman, T., MacDonald, A.L., Pink, D.A. and Zuckermann, M.J. (1983) J. Chem. Phys. 79, 2027–2041.
15 Lookman, T., Pink, D.A., Grundke, E.W., Zuckermann, M.J. and De Verteuil, F. (1982) Biochemistry 21, 5593–5601.
16 Pink, D.A., Lookman, T., MacDonald, A.L., Zuckermann, M.J. and Jan, N. (1982) Biochim. Biophys. Acta 687, 42–56.
17 MacDonald, A.L. and Pink, D.A. (1987) Biochemistry 26, 1909–1917.
18 Hjort Ipsen, J., Karlström, G., Mouritsen, O.G., Wennerström, H. and Zuckermann, M.J. (1987) Biochim. Biophys. Acta 905, 162–172.
19 Mouritsen, O.G. (1983) Biochim. Biophys. Acta 731, 217–221.
20 Mouritsen, O.G. and Zuckermann, M.J. (1985) Eur. Biophys. J. 12, 75–86.
21 Mouritsen, O.G., Hjort Ipsen, J. and Zuckermann, M.J. (1988) J. Coll. Int. Sci., in press.
22 Mitaku, S. and Date, T. (1982) Biochim. Biophys. Acta 688, 411–421.
23 Hatta, I., Suzuki, K. and Imaizumi, S. (1983) J. Phys. Soc. Jap. 52, 2790–2797.
24 Mitaku, S., Jippo, T. and Kataoka, R. (1983) Biophys. J. 42, 127–144.
25 Ruggiero, A. and Hudson, B. (1988) Biophys. J., in press.
26 Zuckermann, M.J. and Mouritsen, O.G. (1987) Eur. Biophys. J. 15, 77–86.
27 Mouritsen, O.G. (1984) Computer Studies of Phase Transitions and Critical Phenomena, Springer-Verlag, Heidelberg.
28 Benz, R., Beckers, F. and Zimmermann, U. (1979) J. Membr. Biol. 48, 181–204.
29 Benz, R. and Zimmerman, U. (1981) Biochim. Biophys. Acta 640, 169–178.
30 Abidor, I.G., Arakelyan, V.B., Chernomordik, L.V., Chizmadzhev, Y.A., Pastushenko, V.F. and Tarasevich, M.R. (1979) Bioelectrochem. Bioenerg. 6, 37–52.
31 Sugar, I.P. and Neumann, E. (1984) Biophys. Chem. 19, 211–225.
32 Powell, K.T. and Weaver, J.C. (1981) Bioelectrochem. Bioenerg. 15, 211–227.
33 Weaver, J.C., Mintzer, R.A., Ling, H. and Sloan, S.R. (1986) Bioelectrochem. Bioenerg. 15, 229–241.
34 Powell, K.T., Derrick, E.G. and Weaver, J.C. (1986) Bioelectrochem. Bioenerg. 15, 243–255.
35 Lorenzen, S., Servuss, R.-M. and Helfrich, W. (1986) Biophys. J. 50, 565–571.
36 Holzwarth, J.F. (1986) Faraday Discuss. Chem. Soc. 81, 353–367.
37 Carruthers, A. and Melchior, D.L. (1983) Biochemistry 22, 5797–5807.
38 Linden, C.D., Wright, K.L., McConnell, H.M. and Fox, C.F. (1973) Proc. Natl. Acad. Sci. USA 70, 2271–2275.
39 Wu, S.H. and McConnell, H.M. (1973) Biochem. Biophys. Res. Commun. 55, 484–491.
40 Sakanishi, A., Mitaku, S. and Ikegami, A. (1979) Biochemistry 12, 2636–2642.
41 Weiss, R.M. and McConnell, H.M. (1985) J. Phys. Chem. 89, 4453–4459.
42 Cruzeiro, L. and Da Silva, K.M.C. (1985) in Recent Advances in Biological Studies: Structure and Biogenesis, Oxidation and Energetics (Packer, L., ed.), pp. 165–178, Plenum Press, New York.
43 Träuble, H. (1971) J. Membr. Biol. 4, 193–208.
44 Freire, E. and Biltonen, R. (1978) Biochim. Biophys. Acta 514, 54–68.